



Combined OCT distance and FBG force sensing cannulation needle for retinal vein cannulation: in vivo animal validation

M. Ourak¹ · J. Smits¹ · L. Esteveny¹ · G. Borghesan¹ · A. Gijbels¹ · L. Schoevaerds¹ · Y. Douven² · J. Scholtes² · E. Lankenau³ · T. Eixmann⁴ · H. Schulz-Hildebrandt⁴ · G. Hüttmann⁴ · M. Kozlovsky⁵ · G. Kronreif⁵ · K. Willekens⁶ · P. Stalmans⁶ · K. Faridpooya⁷ · M. Cereda⁸ · A. Giani⁸ · G. Staurengi⁸ · D. Reynaerts¹ · E. B. Vander Poorten¹

Received: 27 April 2018 / Accepted: 18 July 2018 / Published online: 28 July 2018
© CARS 2018

Abstract

Purpose Retinal vein cannulation is an experimental procedure during which a clot-dissolving drug is injected into an obstructed retinal vein. However, due to the fragility and minute size of retinal veins, such procedure is considered too risky to perform manually. With the aid of surgical robots, key limiting factors such as: unwanted eye rotations, hand tremor and instrument immobilization can be tackled. However, local instrument anatomy distance and force estimation remain unresolved issues. A reliable, real-time local interaction estimation between instrument tip and the retina could be a solution. This paper reports on the development of a combined force and distance sensing cannulation needle, and its experimental validation during in vivo animal trials.

Methods Two prototypes are reported, relying on force and distance measurements based on FBG and OCT A-scan fibres, respectively. Both instruments provide an 80 µm needle tip and have outer shaft diameters of 0.6 and 2.3 mm, respectively.

Results Both prototypes were characterized and experimentally validated ex vivo. Then, paired with a previously developed surgical robot, in vivo experimental validation was performed. The first prototype successfully demonstrated the feasibility of using a combined force and distance sensing instrument in an in vivo setting.

Conclusion The results demonstrate the feasibility of deploying a combined sensing instrument in an in vivo setting. The performed study provides a foundation for further work on real-time local modelling of the surgical scene. This paper provides initial insights; however, additional processing remains necessary.

Keywords Retinal vein cannulation · Cannulation needle · Optical coherence tomography · Fibre Bragg grating · Surgical robotics

Mouloud Ourak and Jonas Smits are designated as co-first authors of this work.

✉ M. Ourak
mouloud.ourak@kuleuven.be

- 1 University of Leuven, Leuven, Belgium
- 2 Eindhoven University of Technology, Eindhoven, The Netherlands
- 3 OptoMedical Technologies GmbH, Lübeck, Germany
- 4 Medical Laser Center Lübeck GmbH, Lübeck, Germany
- 5 Austrian Center for Medical Innovation and Technology GmbH, Neustadt, Austria
- 6 University Hospitals Leuven, Leuven, Belgium
- 7 The Rotterdam Eye Hospital, Rotterdam, The Netherlands
- 8 The Eye Clinic, University of Milan, Milan, Italy

Introduction

Retinal vein occlusion

Patients with retinal vein occlusion (RVO) suffer from an obstructed blood flow in the retina [21]. This can lead to severe vision impairing damage due to neovascularization, ischaemia, and oedema [15]. RVO is the second most common retinal vascular disorder after diabetic retinal disease and affects 16.4 million people worldwide [24]. Currently, no curative treatment is clinically available. A promising but very challenging experimental treatment is retinal vein cannulation (RVC) [29]. During such an intervention, the goal is to cannulate the clotted retinal vein, followed by the injection of a clot-dissolving drug to restore blood circulation. This is done using a cannulation instrument containing a micronee-

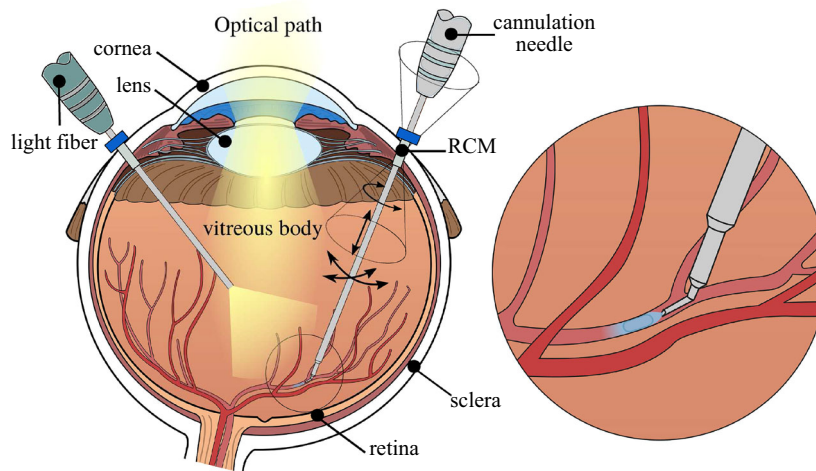


Fig. 1 An annotated overview of key elements during RVO [10]

dle, which is inserted into the eye via a small incision in the sclera (Fig. 1). During the procedure, the surgeon has visual feedback through a stereomicroscope. The illumination of the surgical scene is performed internally, by introducing a light probe, or a pair of optical fibres (i.e. chandeliers) into the eye. Given the minute scale of retinal veins, between 30 and 400 μm , this is an extremely challenging task. Three key challenges can be associated with RVC: (1) guiding the needle to the target vein with an accuracy of 10 μm [23], (2) stopping at the proper depth when puncturing the vein and (3) maintaining the needle position during the injection [12]. Successfully performing these feats relies strongly on the surgeon's capacity to manage undesired hand motion—typically in the order of 300–400 μm [20]—as well as on the degree of local awareness of the target anatomy. Due to these challenges, RVC remains controversial and is not performed in clinical practice today.

Robotic assistance

Several robotic systems for eye surgery have been reported to address the key surgical challenges related to retinal surgery [19]. A distinction between three categories of architectures can be made: telemanipulation, comanipulation and hand-held. Physiological hand tremor is typically managed by means of motion or force scaling. Except for handheld architectures, a shared key functionality is typically the limiting of instrument motion to a single entry point in the sclera [Remote Center of Motion (RCM)] (Fig. 1). Despite the advantages offered by surgical robotics, local estimation of tool-to-surface distance and force remain unresolved problems, resulting in increased surgical risk. Depth estimation is only approximated through the observation of the shadows and the focus of the image on the instrument of the stereomicroscope [7] and is impaired at higher magnifications [6].

Furthermore, instrument-to-surface interaction forces have been confirmed to be below the threshold of human perception during retinal surgery [8,11]. It is clear that an inaccurate perception of the depth and an absence of the force estimate create high surgical risks and is able to induce severe complications [25].

Measuring functions for surgical instruments

A precise local estimation of the interaction between the needle tip and the retina could provide a solution. For this purpose, two measurement methods are envisaged: a proximity sensor and a contact sensor, both located near the end of the cannulation instrument.

Proximity sensing

A significant amount of research has been conducted to allow intraocular detection or distance sensing. Optical coherence tomography (OCT) forms a promising approach, visualizing the anatomical structure along a single ray (A-scan), swept over a line (B-scan) or across a surface (C-scan). OCT provides non-invasive (no contact) information of the retina with micrometre resolution, at rate of few milliseconds for A-scans [7]. Previous research has typically been done relying on two different probe designs.

A lateral-imaging probe measures the tissue at the side of the probe [2]. A recent in-human pilot study including three patients has been reported. For this configuration, the feasibility of defining a retinal structure with acceptable resolution during a peel procedure of the epiretinal membrane has been demonstrated.

A forward-imaging probe measures anatomical structures directly in front of the probe tip. Research dedicated to this type of imaging probe is further developed, as indicated by

the amount of the literature on the topic [3,28]. Different applications show the potential for intraoperative use and control including compensation of physiological motions and retina tracking [28]. Balicki et al. [3] demonstrated on a synthetic phantom how OCT-based distance can be used to set up a virtual wall as a positional safety boundary.

Contact sensing

Instrument to retina interaction forces have been reported to range between 0.6 and 17.5 mN [10] in typical VRS with a possible resolution below 0.25 mN [13]. Previous research on interaction force estimation for retinal surgery has been aimed at preventing the application of excessive force with the instrument, during specific surgical tasks such as RVC and epiretinal membrane peeling [9,14,17]. In addition to surgical safety, intraoperative force data could contribute in identifying mechanical properties of retinal tissue. This information would be useful to build up a more realistic virtual training environments [11].

Different technologies have been proposed to measure the tool-tissue force in vitreoretinal: semiconductor strain gauges [18], microelectromechanical systems-based diffractive optical encoders [30] and intensity-modulated fibre optic sensing [22]. Nevertheless, these methods experience problems in distinguishing contributions from force exerted on the instrument tip and forces that are exchanged at the interface with the sclera. A proposed solution is to integrate the measurement functionality at the tip of the instrument. This imposes additional challenges in terms of biocompatibility, sterilizability and safety.

Fibre Bragg grating (FBG) based on optical fibre provides a solution to these issues. FBG can detect fine changes in strain and thus when paired with a known flexure. FBGs are adequately small sized (diameter of 60–200 μm), inherently safe, biocompatible, sterilizable, relatively inexpensive and highly sensitive. Their output is insulated from electrostatic and electromagnetic noise [1]. Several works in the literature describe how FBGs have been embedded in ophthalmological instruments [9,11,13,17,26].

Objectives

A first effort to combine two sensing modalities to assist RVC was reported in [27]. Hereby, it was shown that relevant distance and force data can be acquired on ex vivo enucleated porcine eyes. However, this conceptual design did not integrate the two sensors within a single instrument. A second version of the instrument was designed and characterized in [26]. This second version combines both sensing modalities in a single instrument and was validated in vitro and ex vivo. This paper provides some insights on the data (force and distance) collected with the instrument for in vivo animal trial.

The experiments were carried out to evaluate the previously developed sensorized instruments. Depth and contact were the major issues, different groups have developed sensors in the past, but there have been very little validated in a realistic in vivo context. With this experiment, we investigate practical issues that may occur. Understanding of the force and damage that occurs may allow developing improved robotic assistance schemes that improve safety and reliability of interactions with the retina. This paper progresses our prior work [26,27] and introduces two prototypes in “Design of a cannulation needle with combined distance and force” section. “Animal trial” section depicts a first animal trial to evaluate the combined sensor in real operation. The performance of the combined OCT distance and FBG force is reported. Finally, conclusion and future perspectives are given in “Conclusion and future work” section.

Design of a cannulation needle with combined distance and force

This section describes the design of a combined force and distance sensing cannulation instruments based on FBG and OCT A-scan technology. Both sensing modalities are briefly described, after which the conceptual designs of two prototypes are presented.

Force sensing

In order to integrate force sensing modality into a cannulation needle, FBG fibres were chosen. An initial design of a 2-DOF force-sensitive needle serves as a basis [9]. In addition to the FBG fibres, a *Micron Optics sm130* interrogator was used, which offers a wavelength detection resolution and scan frequency of, respectively, 2 pm and 500 Hz.

The resulting prototype offers a thermally compensated 1-DOF force measurement, showing negligible drift, and a precision and measurement range of 0.20 and 20 mN, respectively. A detailed overview of the force sensor characterization can be found in [26].

Distance sensing

A custom-made long-range optical distance sensing fibre providing OCT A-scan data, with an outer diameter of 125 μm , was made by Medical Laser Center Lübeck (MLL). The OCT A-scan fibre was connected via an optical switch to an available medical grade iOCT scanner (OptoMedical Technologies (OPMed)). The OCT A-scan fibre was aligned to target a sample with approximately 1–3 mm distal from the needle tip reference. The OCT A-scan data were collected at a sample rate of 200 Hz, at a pixel resolution of 3.8 μm . Precision and accuracy of the distance measurement

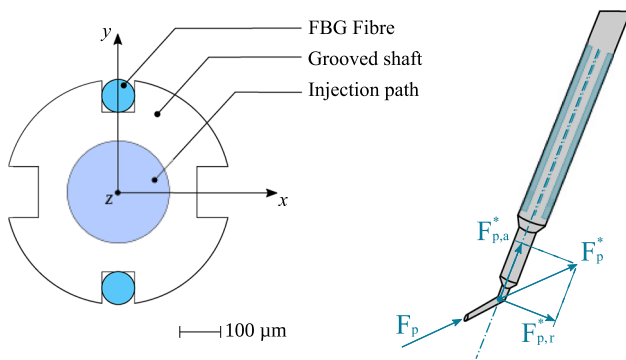


Fig. 2 Conceptual model of the force in the cannulation needle

were characterized at 0.064 and 0.010 mm, respectively, for in vitro samples, at a maximum response time of 0.1 s. A detailed overview of the distance sensor characterization can be found in [26].

Proposed prototypes

Two different configurations have been proposed to evaluate this combination.

A hollow shaft with four parallel grooves acts as a flexure, with the FBG fibres glued into two opposing grooves, and the OCT fibre in one of the other remaining grooves (Fig. 2). These FBG fibres provide strain measurements due to bending in the y direction. Each opposing strain measurement provides an estimate of a radial force component (F_p) along the instrument's y direction applied at the needle tip. The difference between strains provides an estimate that is free of thermal effects.

Shared tube (ST) prototype

STP (Fig. 3) combines all fibres on a single grooved hollow shaft of 0.55 mm outer diameter. The fibres are routed near the tip of the instrument. The main advantages of this design are: ease manufacturing, simplicity and small outer diameter. A limitation is that the OCT fibre is not oriented towards the tip of the needle, but measures the distance at a certain offset, in x and y direction. Therefore, the needle tip is not in the field of view of the OCT A-scan. This requires a pre-calibration of the needle tip location with respect to the OCT fibre. Furthermore, the sensorized tube is directly exposed to the sclera entry point.

Outer sleeve (OS) prototype

OSP (Fig. 4) is composed of an internal part for force measurements and an external part made of an outer sleeve for distance measurements. The assembly is more complex but allows to position the needle tip within the OCT view.

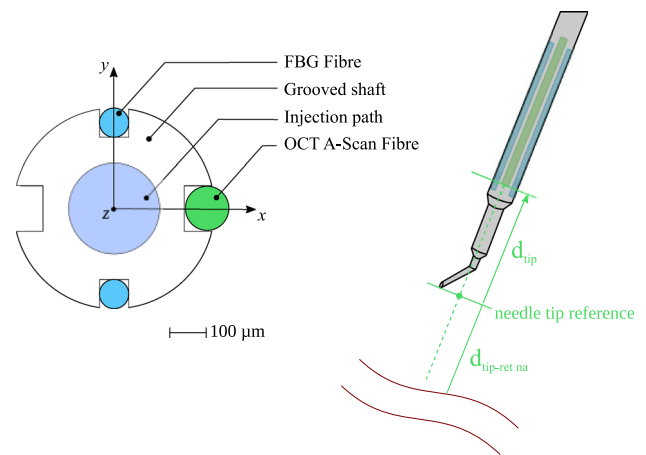


Fig. 3 Conceptual sketch of STP: OCT and FBG fibres are aligned along three grooves in the same shaft

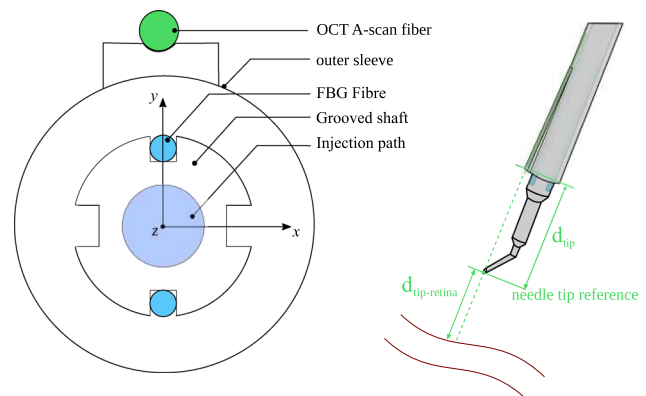


Fig. 4 Conceptual sketch of OSP: OCT and housing surrounds a force sensing cannulation needle

prototype allows collocated force and distance measurement. The outer sleeve shields the force measuring part, protecting the measurement segment from large sclera interaction forces. However, the resulting diameter of the outer sleeve that is to be inserted inside the eye is 2.3 mm with a 0.6 mm protuberance.

Animal trial

The performed animal study was approved by the Ethical Committee for Animal Research at Medanex Clinic. In total, experiments were performed on 3 pigs. Four surgeons from three different institutes participated, taking turns throughout 2 days to perform the experiments. A protocol for the experiments was set up and adhered to. All required equipments were transported to the facility and field-tested beforehand.

A Haag-Streit surgical stereomicroscope (Hi-R NEO 900A NIR) was used, paired with a dedicated iOCT system (OPMedt GmbH). In addition, a fibre OCT A-scan probe



Fig. 5 Operating theatre of animal trial

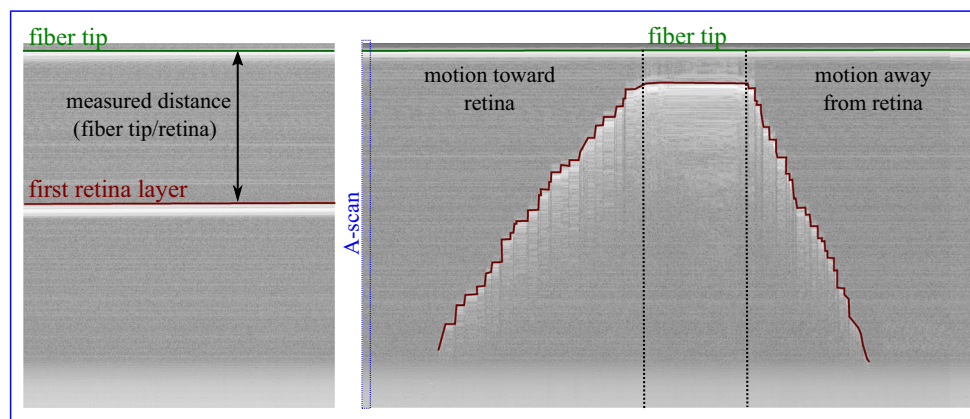


Fig. 6 Distance measurement based on OCT fibre

from MLL embedded within the cannulation needle was plugged into the same OCT system via a purposely developed fibre switch. Force was measured using a Micron Optics *sm130* interrogator connected to a real-time PXI industrial computer from national instruments. Two cannulation needle prototypes were fixed to a previously developed comanipulation surgical robot [10]. For research purposes, surgical robot control was implemented on a real time (Xenomai 6). The hardware of the robot (motors, encoders and two foot pedals) was connected to a national instrument NI9144 EtherCAT slave with embedded FPGA used for data acquisition. The control programme was running on OROCOS a middle-ware for real-time robot control [5].

A general view of the operating theatre at Medanex Clinic facility is provided in Fig. 5. During the animal trial, both prototype needles were tried out for evaluation. Even though suitable for laboratory work, the OS prototype was found infeasible to safely introduce into the eye due to its large outer

diameter (2.3 mm). In the following, only the ST prototype was used and its data depicted.

OCT distance versus insertion depth

The first experiment was conducted to check the quality of the distance measurements with the OCT fibre. The estimation of the distance within the 4 mm possible by the OCT is shown in Fig. 6. The extraction of the distance from the A-scan was based on the work presented in [4] for further details.

Figure 7 depicts the resulting curves of the robot insertion depth motion (translation along the needle axis) and the OCT distance estimation within 4 mm range of the OCT sensor. The OCT distance shows a similarity with the robot insertion depth but not correspondence. This is most likely due to slight bending of the instrument caused by sclera interaction forces, resulting in a measurement mismatch between the robot workspace and local measurement data. In conclusion,

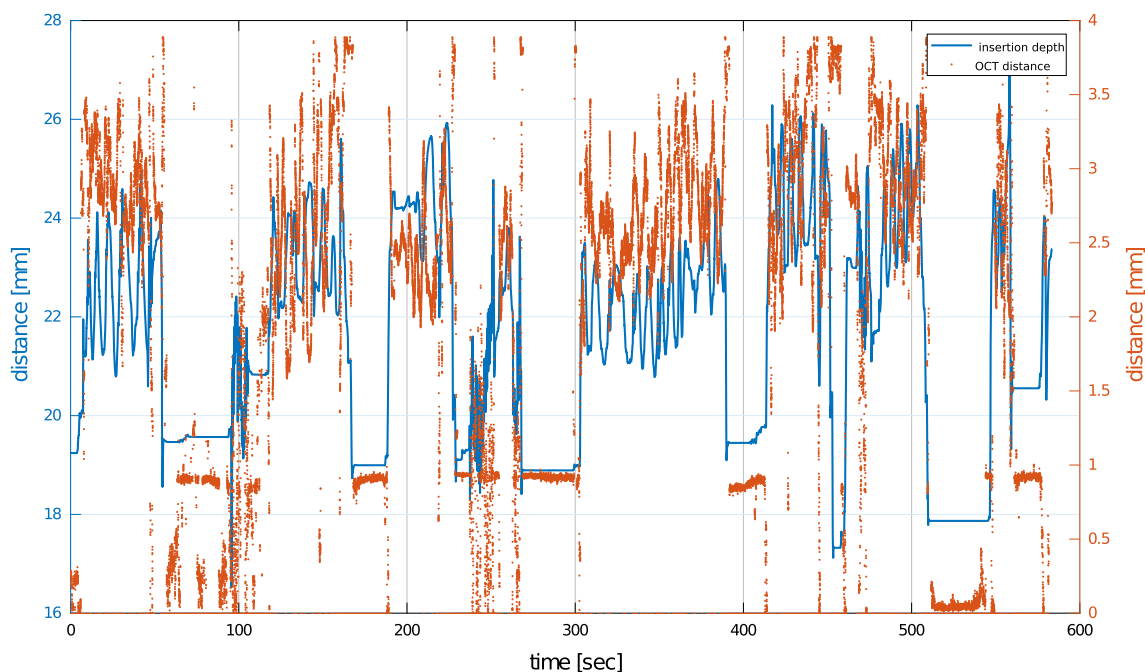


Fig. 7 Evaluation of the OCT distance versus the robot insertion depth motion

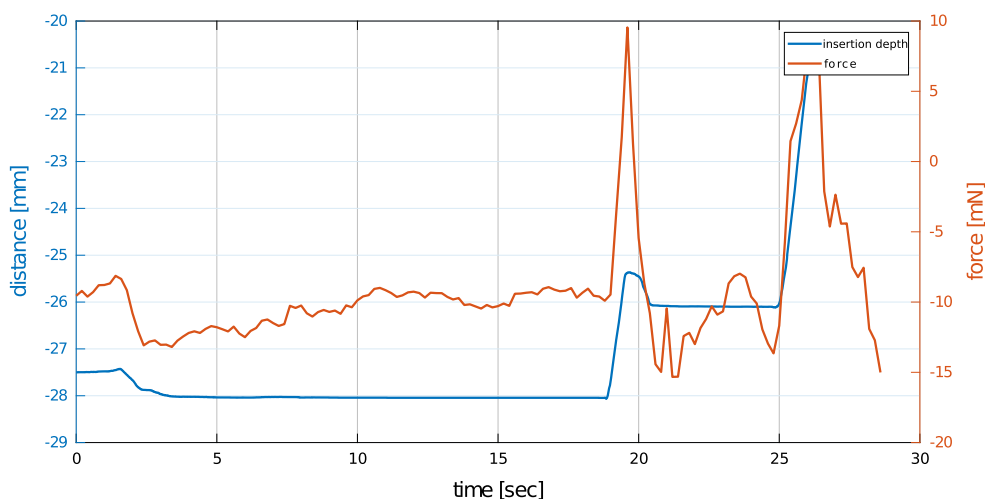


Fig. 8 Evaluation of the force vs. the robot insertion depth motion

the OCT A-scan signal can get a real-time estimate of the distance to the retina surface, but care must be taken to filter and interpret its data. Furthermore, it highlights the challenge of combining both robotic and local measurement data.

Force versus insertion depth

A second experiment was conducted to evaluate the behaviour of the force sensor inside a closed porcine eye. This was the first time—to the knowledge of the authors—that such a test with a FBG sensor was conducted on a closed eye. The sensor allows to measure the force in two directions such as if the

force is applied in opposition to the needle tip, it will decrease and conversely. Continuous contact with the needle on the retina was tested. The curve of the experiment is depicted in Fig. 8. The robot is locked between 5 and 18 s where the insertion depth is constant. The force shows an increase of 2.5 mN in the force measurements. It was observed that this force is caused by eye motion of the sedated animal, assumed to be caused by breathing. This motion is not noticeable from the robot encoders but can be seen on the stereomicroscope. Note when retracting the needle, between 20 and 26 s, noticeable increase of the force can be seen. These forces were observed

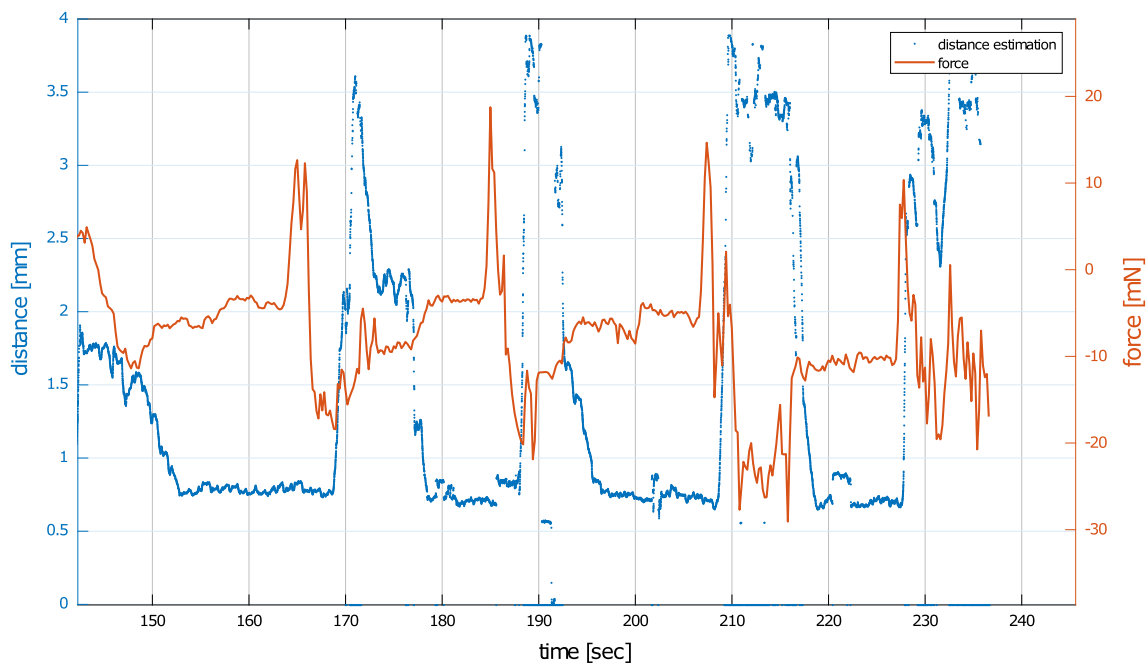


Fig. 9 Evaluation of the force vs. the OCT distance for a short time contact

to be caused by sclera interaction forces during instrument extraction.

Multiple approaches to the retina were made to understand the behaviour of the force sensor in the closed eye. Data of the force and OCT distance were gathered simultaneously during this multiple contact approach. Figure 9 depicts the evolution of the two signals. Between 155 and 165 s the distance does not change, yet a force peak is seen. This variation of the force is related to the physiological motion that will be demonstrated in the next subsection. Between 165 and 175 s, the surgeon is retracting the robot and a force peak in the same direction is measured.

STP was able to measure forces inside the eye. The values of the force were between + 20 and – 20 mN for the different experiments. The continuous contact shows the possible use of the force to estimate the force at the needle tip even when such is not easily noticed with the distance measurement. However, even though not directly measured, a clear correlation between robot motion and force measurements can be observed. Furthermore, when purposefully misaligning the surgical robot with the sclera entry point, this correlation was observed to scale up. It is concluded that this correlation is caused by the direct interaction between the fibres in the grooved tube and the trocar at the sclera entry. This highlights a key design concern for the usage of FBG fibre-based through a trocar, as this requires some form of mechanical isolation for the bare, non-measuring section of the fibres. This could be achieved as proposed in the OS prototype, using a stiff outer tube concept.

Acquisition of physiological motion

Physiological motion caused by breathing and the heartbeat could be observed by using the OCT distance estimation. The breathing motion depicted in Fig. 10 approximates a sinusoidal trajectory. The breathing frequency was approximately 11 breaths per minute. Moreover, the effect of the heartbeat was visible as a small variation superpositioned on the sinusoidal motion at approximately 120 heartbeats per minute. Peak-to-peak position amplitudes are observed to be approximately 0.1 and 0.3 mm for motions caused by heartbeat and breathing, respectively.

The force sensor was used to measure the physiological motion. Figure 10 shows the evolution of the OCT distance measurement for a constant insertion depth and for different positions on the retina. From the graph we see that also when in contact the distance measurement works as well. The corresponding force signal is depicted in Fig. 10. Even though slightly scaled down, the force sensor continues to clearly depict the physiological forces when not in direct contact with the retina. This confirms the earlier made conclusion of force interference due to sclera interaction forces.

Conclusion and future work

This paper presented two designs of sensorized cannulation needles enabling combined force and distance sensing. The first results of in vivo porcine animal experiments are reported. For both prototypes, the force measurement relies

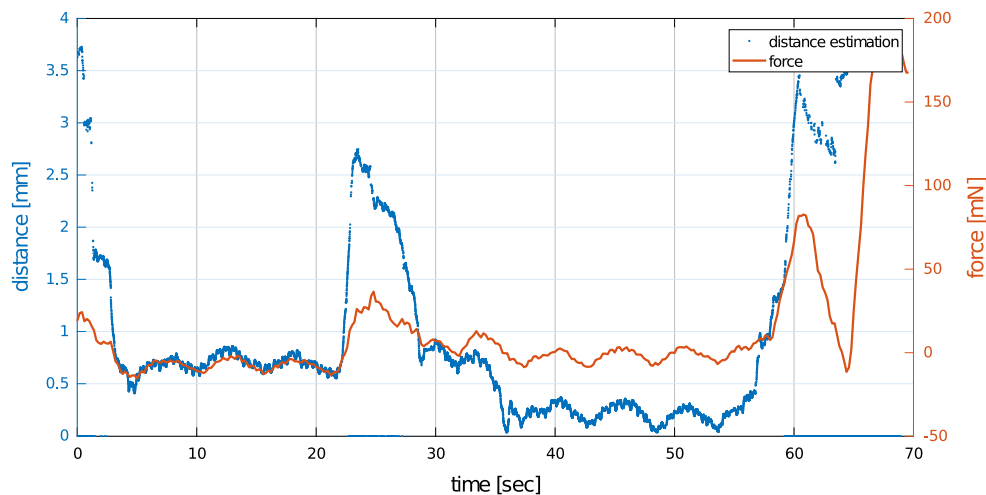


Fig. 10 Evaluation of force vs. robot insertion depth motion for the estimation of the physiological motion

on two FBG fibres that are glued on a custom 0.6 mm-diameter hollow flexure. The distance measurement that relies on an integrated OCT fibre is used. Two different layouts have been investigated here. In STP, the same shaft of the cannulation needle is employed, leading to a small outer diameter of 0.6 mm, providing non-collocated force and distance sensing. In OSP, OCT fibre is embedded in a separate construction leading to a collocated measurement, but resulting in a large outer diameter of 2.3 mm. A characterization and calibration of the two prototypes was conducted. In order to validate the feasibility of using such sensorized instrument in an *in vivo* setting, an animal trial campaign was conducted at Medanex Clinic facility. During these experiments, surgeons validated the OCT A-scan probe distance estimation technology, in order to enable future robot-assisted procedures within the context of an initial *in vivo* human study. At the same time, these experiments were conducted to further validate the functioning of the combined OCT and force sensing cannulation needles. Within this effort, a unique data set was gathered of *in vivo* OCT and force sensing.

Whereas both instruments (ST and OS) worked well in a laboratory setting, it was found that the larger outer diameter OS concept was not feasible in an *in vivo* setting. Surgeons managed to successfully use the ST prototype throughout the preconceived experimental protocol. A key observation was that a clear coupling between force measurements and sclera interaction forces was observed. This highlights the need for a reliable mechanical decoupling of the present fibres from the sclera entry. Despite this setback, valuable force and OCT data were able to be measured and is still being processed. Intraoperative retinal motion due to heartbeat and breathing motion was found to be in the order of 0.1 and 0.3 mm, respectively. To the knowledge of the authors, this has been the first time that such a combined force/OCT cannulation needle was tested *in vivo*. Valuable insights have been obtained, which

will form the foundation for future work on the development of improved smart surgical instrumentation.

Funding This research was funded by the EU Framework Programme for Research and Innovation-Horizon 2020 (No. 645331) and an SB Fellowship of the Research Foundation-Flanders (1S41517N).

Compliance with ethical standards

Conflict of interest The authors declare that they have no conflict of interest.

Ethical approval This article does not contain any studies with human participants performed by any of the authors. All applicable international, national, and/or institutional guidelines for the care and use of animals were followed.

Informed consent This articles does not contain patient data.

References

1. Ambastha S, Umesh S, Dabir S, Asokan S (2016) Spinal needle force monitoring during lumbar puncture using fiber Bragg grating force device. *J Biomed Opt* 21(11):117002
2. Asami T, Terasaki H, Ito Y, Sugita T, Kaneko H, Nishiyama J, Namiki H, Kobayashi M, Nishizawa N (2016) Development of a fiber-optical coherence tomography probe for intraocular use. *Investig Ophthalmol Vis Sci* 57(9):OCT568–OCT574
3. Balicki M, Han Jh, Iordachita I, Gehlbach P, Handa J, Taylor R, Kang J (2009) Single fiber optical coherence tomography microsurgical instruments for computer and robot-assisted retinal surgery. In: *Medical image computing and computer-assisted intervention*, pp 108–115
4. Borghesan G, Ourak M, Lankenau E, Hüttmann G, Schulz-Hildebrandt H, Willekens K, Stalmans P, Reynaerts D, Vander Poorten E (2018) Single scan OCT-based retina detection for robot-assisted retinal vein cannulation. *J Med Robot Res* 3(02):1840005
5. Bruyninckx H, Soetens P, Koninckx B (2003) The real-time motion control core of the Orocos project. In: *IEEE international conference on robotics and automation*, vol 2, pp 2766–2771

6. Du LT, Wessels IF, Underdahl JP, Auran JD (2001) Stereoacuity and depth perception decrease with increased instrument magnification: comparing a non-magnified system with lens loupes and a surgical microscope. *Binocul Vis Strabismus Q* 16(1):61–7
7. Ehlers JP, Srivastava SK, Feiler D, Noonan AI, Rollins AM, Tao YK (2014) Integrative Advances for OCT-guided ophthalmic surgery and intraoperative OCT: microscope integration, surgical instrumentation, and heads-up display surgeon feedback. *PLoS ONE* 9(8):e105224
8. Ergeneman O, Pokki J, Počepcovà V, Hall H, Abbott JJ, Nelson BJ (2011) Characterization of puncture forces for retinal vein cannulation. *J Med Devices* 5(4):044504
9. Gijbels A, Vander Poorten EB, Stalmans P, Reynaerts D (2015) Development and experimental validation of a force sensing needle for robotically assisted retinal vein cannulations. In: *IEEE international conference on robotics and automation*, pp 2270–2276
10. Gijbels A, Willekens K, Esteveny L, Stalmans P, Reynaerts D, Vander Poorten EB (2016) Towards a clinically applicable robotic assistance system for retinal vein cannulation. In: *IEEE international conference on biomedical robotics and biomechanics*, pp 284–291
11. Gonenc B, Chamani A, Handa J, Gehlbach P, Taylor R, Iordachita I (2017) 3-DOF force-sensing motorized micro-forceps for robot-assisted vitreoretinal surgery. *IEEE Sens* 17(11):3526–3541
12. Gonenc B, Iordachita I (2016) FBG-based transverse and axial force-sensing micro-forceps for retinal microsurgery. In: *IEEE sensors*
13. Gonenc B, Taylor RH, Iordachita I, Gehlbach P, Handa J (2014) Force-sensing microneedle for assisted retinal vein cannulation. In: *IEEE sensors proceedings*, pp 698–701
14. Gonenc B, Tran N, Riviere CN, Gehlbach P, Taylor RH, Iordachita I (2015) Force-based puncture detection and active position holding for assisted retinal vein cannulation. In: *IEEE/SICE/RSJ international conference on multisensor fusion and integration for intelligent systems*, pp 322–327
15. Hayreh SS, Zimmerman MB, Podhajsky P (1994) Incidence of various types of retinal vein occlusion and their recurrence and demographic characteristics. *Am J Ophthalmol* 117(4):429–441
16. He X, Handa J, Gehlbach P, Taylor RH, Iordachita I (2014) A sub-millimetric 3-DOF force sensing instrument with integrated fiber bragg grating for retinal microsurgery. *IEEE Trans Biomed Eng* 61(2):522–534
17. Iordachita I, Sun Z, Balicki M, Kang JU, Phee SJ, Handa J, Gehlbach P, Taylor R (2009) A sub-millimetric, 0.25 mN resolution fully integrated fiber-optic force-sensing tool for retinal microsurgery. *Int J Comput Assist Radiol Surg* 4(4):383–390
18. Menciassi A, Eisinberg A, Sculari G, Anticoli C, Carrozza M, Dario P (2001) Force feedback-based microinstrument for measuring tissue properties and pulse in microsurgery. In: *IEEE international conference on robotics and automation*, vol 1, pp 626–631
19. Molaei A, Abedloo E, de Smet MD, Safi S, Khorshidifar M, Ahmadi H, Khosravi MA, Daftarian N (2017) Toward the art of robotic-assisted vitreoretinal surgery. *J Ophthalmic Vis Res* 12:175–182
20. Noda Y, Ida Y, Tanaka S, Toyama T, Roggia MF, Tamaki Y, Sugita N, Mitsuishi M, Ueta T (2013) Impact of robotic assistance on precision of vitreoretinal surgical procedures. *PLoS ONE* 8:1–6
21. Olver J, Cassidy L (2005) *Ophthalmology at a glance*. Blackwell Science, Hoboken
22. Peirs J, Clijnen J, Reynaerts D, Brussel HV, Herijgers P, Corteville B, Boone S (2004) A micro optical force sensor for force feedback during minimally invasive robotic surgery. *Sens Actuators A* 115(2–3):447–455
23. Riviere C, Ang WT, Khosla P (2003) Toward active tremor canceling in handheld microsurgical instruments. *IEEE Trans Robot Autom* 19:793–800
24. Rogers S, McIntosh RL, Grad B, Journ D, Cheung N, Lim L, Wang JJ, Mitchell P, Kowalski JW, Nguyen H, Wong TY (2011) The prevalence of retinal vein occlusion: pooled data from population studies from the United States, Europe, Asia, and Australia. *Popul Stud* 117:1–14
25. Sjaarda RN, Glaser BM, Thompson JT, Murphy RP, Hanham A (1995) Distribution of iatrogenic retinal breaks in macular hole surgery. *Ophthalmology* 102(9):1387–1392
26. Smits J, Mouloud O, Gijbels A, Esteveny L, Borghesan G, Schoevaerds L, Willekens K, Stalmans P, Lankenau E, Schulz-Hildebrandt H, Hüttmann G, Reynaerts D, Vander Poorten, E (2018) Development and experimental validation of a combined FBG force and OCT distance sensing needle for robot-assisted retinal vein cannulation. In: *IEEE international conference on robotics and automation*
27. Smits J, Ourak M, Gijbels A, Borghesan G, Esteveny L, Schoevaerds L, Willekens K, Stalmans P, Lankenau E, Hüttmann G, Reynaerts D, Poorten EBV (2017) Combined force and distance sensing for robot-assisted vitreo-retinal surgery. In: *Proceedings of the 7th joint workshop on new technologies for computer/robot assisted surgery*
28. Song C, Gehlbach PL, Kang JU (2012) Active tremor cancellation by a “smart” handheld vitreoretinal microsurgical tool using swept source optical coherence tomography. *Opt Express* 20(21):23414–23421
29. Tang WM, Han DP (2000) A study of surgical approaches to retinal vascular occlusions. *Arch Ophthalmol* 118(1):138–43
30. Zhang X (2004) Silicon microsurgery-force sensor based on diffractive optical MEMS encoders. *Sensor Rev* 24(1):37–41